QSAR & Combinatorial Science QCS

Molecular Docking and 3-D QSAR Studies of Substituted 2,2-Bisaryl-Bicycloheptanes as Human 5-Lipoxygenase-Activating Protein (FLAP) Inhibitors

Xiang Ma[a], Lu Zhou[a]*, Zhi-Li Zuo[b], Jian Liu[a], Min Yang[a] and Rong-Wei Wang[a]

[a] Department of Pharmaceutical Engineering, College of Chemical Engineering, Sichuan University, Sichuan, Chengdu 610065, China, E-mail: zhouluscu@163.com
[b] Centre for Biomedical and Life Sciences, Singapore Polytechnic, 139651 Singapore, Singapore

Keywords: CoMFA, 3-D QSAR, 5-Lipoxygenase-Activating Protein (FLAP), Molecular docking, Substituted 2,2-bisaryl-bicycloheptanes
Revised: July 15, 2008

Received: May 10, 2008; Accepted: July 19, 2008

DOI: 10.1002/qsar.200810053

Abstract
Leukotrienes have been shown to be involved in a variety of diseases such as cardiovascular diseases, cancer, asthma, ulcerative colitis, and rhinitis. 5-Lipoxygenase-Activating Protein (FLAP) was found to be a key enzyme of leukotriene synthesis. Comparative Molecular Field Analysis (CoMFA) and molecular docking studies were carried out on a series of substituted 2,2-bisaryl-bicycloheptanes FLAP inhibitors. The docking results provided a reliable conformational alignment scheme for 3-D QSAR model. Based on the docking conformations, highly predictive CoMFA model was performed with a leave-one-out cross-validated q^2 of 0.651. The noncross-validated analysis with four optimum components revealed a conventional r^2 value of 0.972, $F=175.674$, and an estimated standard error of 0.169. The predictive ability of this model was validated by the testing set with a conventional r^2 value of 0.920. The analyses may be used to design more potent FLAP inhibitors and predict their activities prior to synthesis.

1 Introduction

Leukotrienes have been shown to be involved in a variety of diseases such as cardiovascular diseases, cancer, asthma, ulcerative colitis, and rhinitis [1–3]. Cellular activation by immune complexes and other inflammatory stimuli result in an increase in intracellular calcium and the translocation of Cytosolic Phospholipase A_2 (cPLA$_2$) and 5-Lipoxygenase (5-LO) from the cytosol to the nuclear membrane [4]. Membrane-embedded FLAP selectively transfers AA to 5-LO and enhances the sequential oxygenation of AA to 5(S)-Hydroperoxyeicosatetraenoic acid (5-HpETE) and dehydration to Leukotriene A4 (LTA$_4$) [5]. LTA$_4$ can then be exported from the cell for transcellular metabolism or converted either to pro-inflammatory LTB$_4$ or to the bronchoconstrictive, vasoconstrictive, and pro-inflammatory cysteinyl leukotrienes (CysLTs), namely LTC$_4$, LTD$_4$, and LTE$_4$ [1]. Leukotriene synthesis is a tightly controlled process, and excess AA is reacylated rapidly into membrane phospholipid pools [6]. These are the only known roles for FLAP, and cellular leukotriene synthesis can be completely inhibited by compounds that bind to FLAP [7].

Although there is a plethora of COX inhibitors, known as Non-Steroidal Anti-Inflammatory Drugs (NSAIDs), and the pros and cons of COX-1 *versus* COX-2 inhibitors have been widely debated, there are many fewer marketed modulators of the pro-inflammatory leukotriene pathway. Leukotrienes have physiological roles in innate immune defense, the homeostatic function for which inflammation evolved, and several studies have shown a role for leukotrienes in antimicrobial host defense [8]. Leukotrienes have pathophysiological roles in respiratory diseases, allergic diseases, and Cardiovascular Diseases (CVDs) and there is an excellent recent review on leukotrienes and mechanisms of disease [1]. So, the development of more potent FLAP inhibitors is of great significance.

A number of FLAP inhibitors have appeared in the primary literature [9]. The binding model of inhibitor MK-591 has been determined by X-ray crystallography. The crystal structure provided not only insights into the interaction mechanisms of FLAP with the inhibitor, but also valuable clues for designing new inhibitors [10]. In this paper, with the molecular docking and Three-Dimensional (3-D) QSAR (CoMFA) analyses, it is possible to get new

insights into the relationship between the structural information of the series of 31 substituted 2,2-bisaryl-bicycloheptanes inhibitors and the inhibitory potency, aimed at identifying structural features in FLAP that can be used to find new inhibitors.

2 Computational Details

2.1 Biological Data and Molecular Structures

Thirty-one substituted 2,2-bisaryl-bicycloheptanes inhibitors from one laboratory reported by Dwight *et al.* were gathered [9]. The biological data (represented as IC_{50} values) of these inhibitors were determined under the same experimental conditions. The biological data were considered comparable and divided into a training set and a testing set as shown in Table 1. The training set which were selected randomly consists of 25 compounds and the testing set is comprised of 6 compounds. The IC_{50} values were converted into pIC_{50} (Eq. (1)). The pIC_{50} were then used for subsequent QSAR analysis as the response variable.

$$pIC_{50} = -\lg IC_{50} \quad (1)$$

The 3-D structure of the 31 substituted 2,2-bisaryl-bicycloheptanes were constructed by using molecular modeling software package SYBYL. Partial atomic charges were calculated by the Gasteigere – Hückel method and energy minimizations were performed using the Tripos force field with a distance-dependent dielectric and the Powell conjugate gradient algorithm (convergence criterion of 0.005 kcal/mol/Å) [11].

2.2 Docking Studies

To find the binding model of the inhibitors to the FLAP, the advanced molecular docking program GOLD, version 3.0.1, which uses a powerful Genetic Algorithm (GA) method for conformational search and docking programs, was employed to generate an ensemble of docked conformations. Atomic coordinates for the FLAP complex with MK-591, used for our modeling, have been deposited in the Brookhaven Protein DataBank (PDB ID:2Q7M) [10]. The original ligand was removed from the coordinated set. The genetic operators were 100 for the population size, 1.1 for the selection, 5 for the number of subpopulations, 100 000 for the maximum number of genetic applications, and 2 for the size of the niche used to increase population diversity. The weights were chosen so that crossover mutations were applied with equal probability (95/95 for the values) and migration was applied 5% of the time. ChemScoring function encoded in GOLD was applied to predict binding positions between FLAP and 31 inhibitors. This scoring function was described by Eldridge *et al.* [12, 13]. The fitness score is taken as the negative of the sum of the component energy terms, so that larger fitness scores are better [14].

2.3 Structural Alignment

Molecular alignment is the most sensitive parameter in 3-D QSAR analysis. This renders the spatial alignment of molecules under study as one of the most sensitive and determining factors in obtaining robust and meaningful models. In this study, ten conformations were obtained through GOLD for each inhibitor. Twenty-five inhibitors were selected randomly as the training set, and these inhibitors were aligned together for CoMFA study to explore the specific contributions of electrostatic and steric effects of the molecular bioactivities. The conformations for each ligand of the testing set were chosen to have lowest residues between actual and predicted pIC_{50}, which was predicted by the CoMFA model of the training set.

2.4 CoMFA

Steric and electrostatic interactions were calculated using the Tripos force field [15] with a distance-dependent dielectric constant at all intersections in a regularly spaced (2 Å) grid taking an sp^3 carbon atom as steric probe and a +1 charge as electrostatic probe. The cut off value was set to 30 kcal/mol. With standard options for scaling of variables, the regression analysis was carried out using the Leave-One-Out (LOO) cross-validated Partial Least Squares (PLS) method [16]. The column filtering was set to 2.0 kcal/mol to improve the signal-to-noise ratio by omitting those lattice points whose energy variation was below this threshold. The final model, noncross-validated conventional analysis, was developed with the optimum number of components to yield a noncross-validated r^2 value.

3 Results and Discussion

3.1. Docking Study and Structural Alignment

In order to check the capacity of the parameters set for docking to reproduce the X-ray structure, the ligand MK-591 extracted from crystal structure was redocked to FLAP using GOLD. Figure 1 shows the conformational superposition of the ligand MK-591 and its best docking conformation, the Root Mean Square Deviation (RMSD) between the two conformations is equal to 0.79 Å, indicating that the parameters set for docking were capable of reproducing the X-ray structure. To locate the appropriate binding orientations and conformations of these substituted 2,2-bisaryl-bicycloheptanes inhibitors interacting with FLAP, compound **2** with the highest FLAP binding affinity was docked to FLAP using Surflex and GOLD, respectively. The RMSD between the two best docking conforma-

Table 1. Structures, experimental activities (Obs.), predicted activities (Calcd.), residuals (Res.) by CoMFA model, and docking ChemScores of FLAP inhibitors.

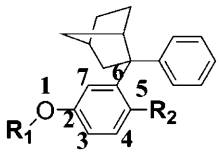

Compound	R_1	R_2	FLAP IC_{50} (nM)	pIC_{50}			ChemScore
				Obs	Calcd	Res	
2	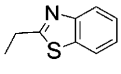	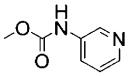	2.5	8.60	8.61	−0.01	46.17
11	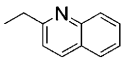	−OH	13.2	7.88	7.64	0.24	41.08
12a	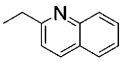	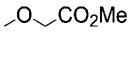	5.0	8.30	8.21	0.09	42.58
12b[a)]	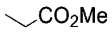	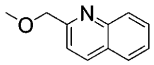	94	7.03	7.70	−0.67	42.46
12c	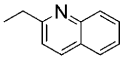	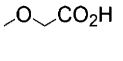	14	7.85	7.79	0.06	42.17
12d		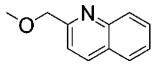	3155	5.50	5.63	−0.13	37.03
12e	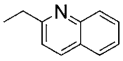	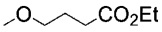	3.7	8.43	8.45	−0.02	44.90
12f	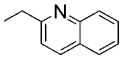	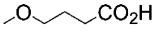	3.5	8.46	8.71	−0.25	43.97
12g	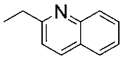		8.6	8.07	8.06	0.01	42.37
12h[a)]	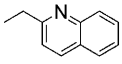		6	8.22	8.27	−0.05	45.07
12i	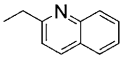	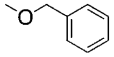	8.6	8.07	8.25	−0.18	46.30
12j	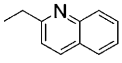	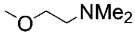	6.5	8.19	8.19	0	44.17
12k[a)]	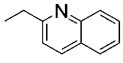	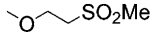	5.5	8.26	8.28	−0.02	42.19
12l	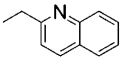	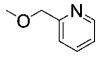	4.1	8.39	8.40	−0.10	45.94
12m		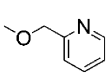	18.3	7.74	7.45	0.29	40.36
12n		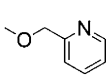	134	6.87	7.11	−0.24	40.81
12o		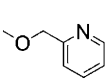	181	6.74	6.93	−0.19	37.59

Table 1. (cont.)

Compound	R_1	R_2	FLAP IC_{50} (nM)	pIC_{50}			ChemScore
				Obs	Calcd	Res	
	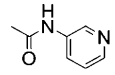						
12p	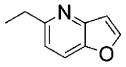	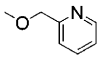	4.9	8.31	8.25	0.06	45.14
12q	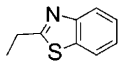	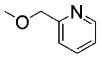	7.6	8.11	8.12	−0.10	43.41
12r	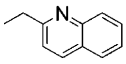	$-CO_2Me$	5.6	8.25	8.42	−0.17	39.28
12s	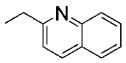	$-CO_2H$	12.4	7.91	7.90	0.01	39.64

Compound	Structure	FLAP IC_{50} (nM)	pIC_{50}			ChemScore
				Obs.	Calcd.	Res.
13	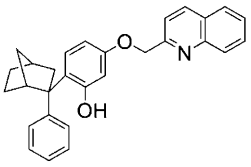	980	6.01	5.94	0.07	37.83
14a[a)]	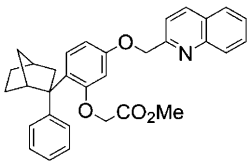	776	6.11	6.67	−0.56	38.03
14b	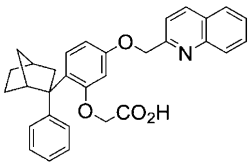	3595	5.44	5.43	0.01	35.21
17	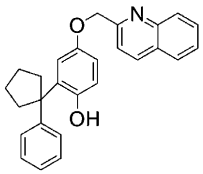	22	7.66	7.52	0.14	40.15
18a	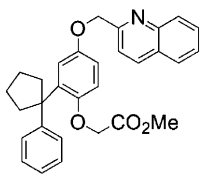	9.3	8.03	8.04	−0.1	39.03

Table 1. (cont.)

Compound	Structure	FLAP IC_{50} (nM)	pIC_{50}			ChemScore
				Obs.	Calcd.	Res.
18b[a)]	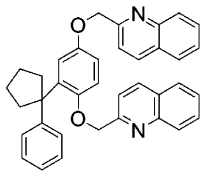	4.5	8.35	8.05	0.30	47.88
18c	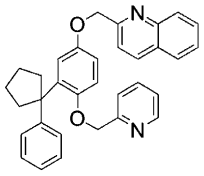	2.5	8.60	8.29	0.31	45.62
18d	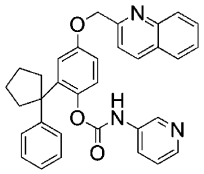	2.4	8.61	8.60	0.01	43.90
18e[a)]	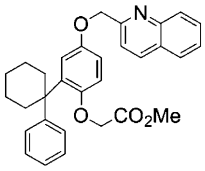	3.7	8.43	8.24	0.19	44.56
18f	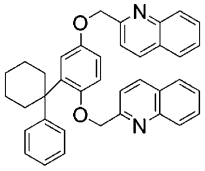	4.2	8.38	8.32	0.06	47.08

[a]Testing set molecules.

tions derived from Surflex and GOLD is equal to 1.11 Å (Figure 2). The two binding conformations are similar with MK-591 extracted from the crystal structure, and the conformation of compound **2** derived from GOLD can be considered as the template for selecting docking conformations of all the other inhibitors derived from GOLD. The predicted binding free energies (ChemScore) for all the inhibitors are listed in Table 1. A linear regression analysis reveals good correlations between the experimental inhibitory activities (pIC_{50}) of the inhibitors and the predicted ChemScore to the FLAP, the r^2 value is equal to 0.64 (Eq. 2 and Figure 3). These correlations demonstrate that the binding conformations and binding models of the inhibitors to FLAP are reasonable

$$pIC_{50} = -1.67 + 0.223\ \text{ChemScore}\ (n = 31,\ r^2 = 0.64,\ F = 51.44,\ s = 0.56) \quad (2)$$

The other 30 molecular conformations possessing high ChemScores and similar conformations with compound **2** were extracted from the inhibitor-FLAP complexes. Figure 4 shows the 3-D model of the 31 substituted 2,2-bisaryl-bicycloheptanes inhibitors at the active sites of FLAP and Figure 5 illustrates the probable binding conformational alignment for the the 31 substituted 2,2-bisaryl-bicycloheptanes inhibitors chosen from the docked conformations. All of the inhibitors are bonded in the active sites of FLAP in a similar conformation with compound **2**, and the common structures superimposed each other well. Based on this set of binding conformations and their alignment, CoMFA model was performed.

In addition, Figure 6 represents the interaction model of the docked inhibitor **12f** with FLAP. Inhibitor **12f** binds to the active site and makes several interactions with FLAP. As shown in the figure, inhibitor **12f** can form hydrogen

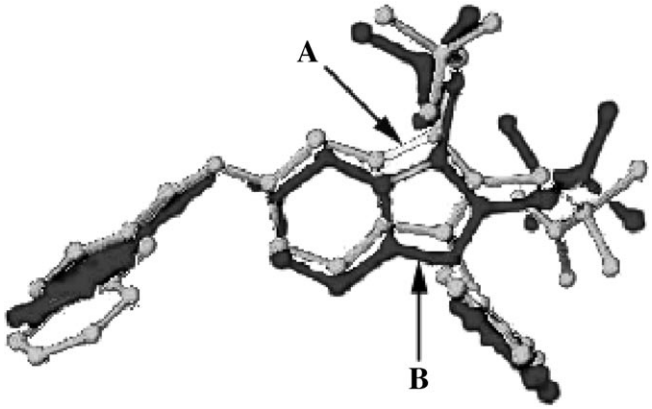

Figure 1. Conformational comparison of MK-591 from the crystal structure of (A) FLAP and (B) that from the docking calculation.

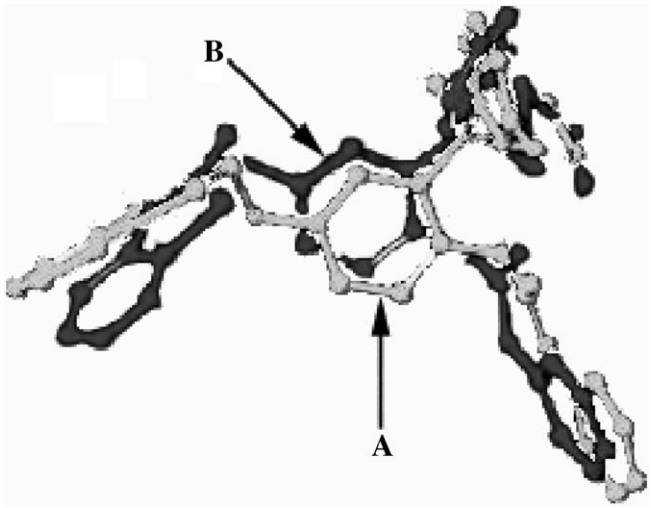

Figure 2. Conformational comparison of compound **2** derived from (A) Surflex and (B) GOLD.

bonds (white dashed lines) with His28 and Lys116. The phenyl ring A interacts with the hydrophobic surface of the side chain of Gly24. The bicycloheptane ring C interacts with the hydrophobic surface of the side chains of Val21, Val20, Phe123, and Ile119. The phenyl ring B interacts with the hydrophobic surface of the side chain of Leu120. The quinoline ring interacts with residue N23, D62, and T66 and weak polar interactions are formed.

3.2 CoMFA Model

Twenty-five of 31 substituted 2,2-bisaryl-bicycloheptanes inhibitors were randomly picked up as training set for constructing CoMFA models, the remaining six inhibitors were used as testing set for the model validation. PLS analysis was carried out for the 25 binding conformations, and the results are listed in Table 2, which shows that a

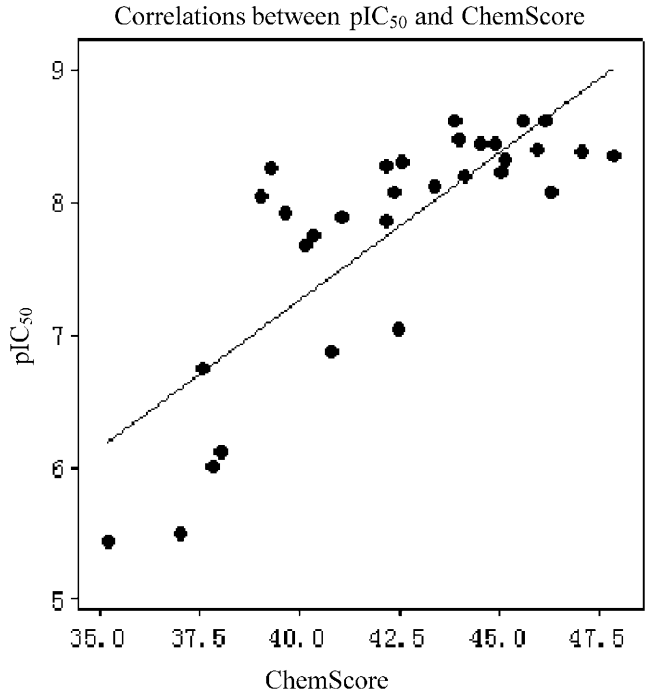

Figure 3. Correlation between the predicted binding free energies (ChemScore) and the experimental activities (pIC_{50}).

Figure 4. Binding conformations of docking compounds at the active sites of FLAP.

CoMFA model with LOO cross-validated q^2 of 0.651 for four components was obtained, and the Standard Error of Prediction (SEP) value is equal to 0.602. The noncross-validated PLS analysis with the optimum components of four resulted in a conventional r^2 of 0.972, $F = 175.674$, and an estimated standard error of 0.169. The steric field descriptors explain 48.7% of the variance, while the electrostatic descriptors explain 51.3%. The predicted activities for the 31 inhibitors *versus* their experimental activities with their

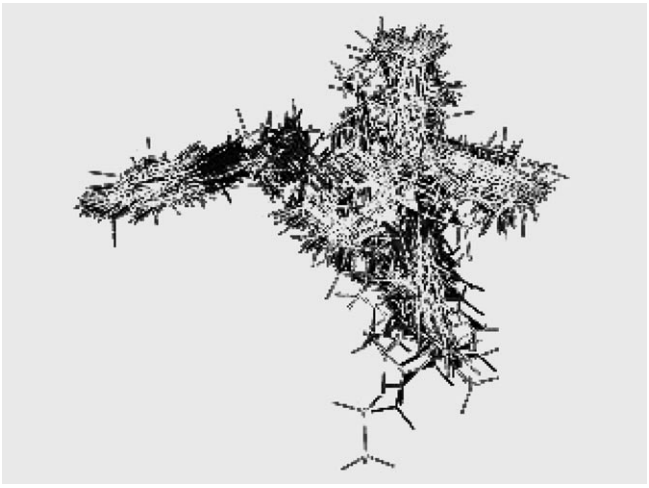

Figure 5. Superimposition of 31 substituted 2,2-bisaryl-bicycloheptanes for 3-D QSAR studies.

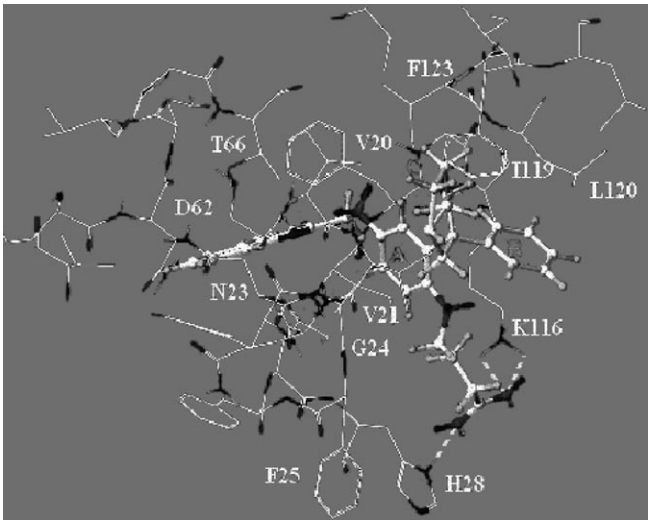

Figure 6. Position of docked inhibitor **12f** in the binding pocket of FLAP. H-bonds and interactions between **12f** and side chain residues.

residues are listed in Table 1. The correlation between the predicted activities and the experimental activities is depicted in Figure 7. Table 2 and Figure 7 demonstrate that the predicted activities by the constructed CoMFA model are in good agreement with the experimental data, suggesting that a reliable CoMFA model was successfully constructed.

The CoMFA contour map of steric contribution is depicted in Figure 8, template compound **18c** was treated as the reference molecule. The green and yellow polyhedra describe regions of space around the molecules where an increase in steric bulk enhances or diminishes the activity, respectively. The electrostatic contribution of CoMFA is illustrated in Figure 9, template compound **12f** was treated as the reference molecule. The blue contour defines a region where increasing positive charge will result in increased activity, whereas the red contour defines a region of space where increasing electron density is favorable.

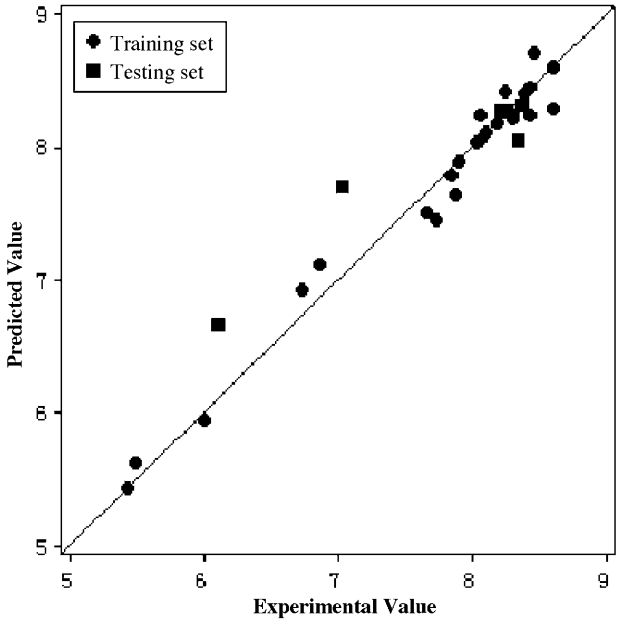

Figure 7. Correlation between predicted activities by CoMFA model and the experimental pIC_{50} values of training and testing sets.

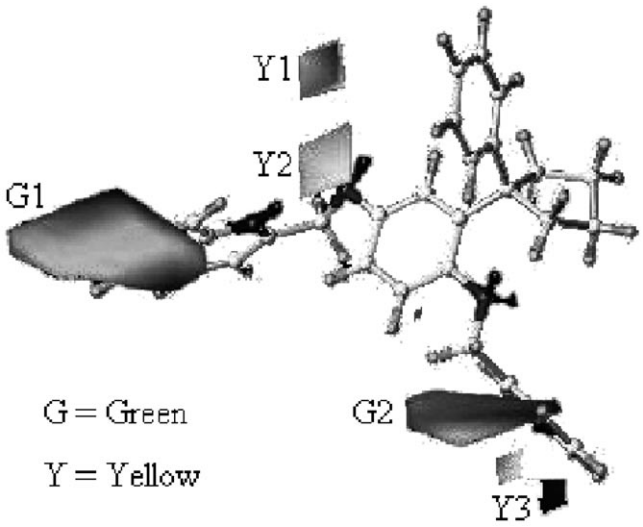

Figure 8. CoMFA steric field distribution contour map in combination with inhibitor **18c.**

In Figure 8, the green contour G1 at the left of the quinoline ring indicates that steric bulk is favored there. As shown in Figure 4, the steric bulk of quinoline and benzothiazole is larger enough to fill up the pocket than pyridine and they have higher electron density than pyridine, and stronger van der Waals interactions might form with resi-

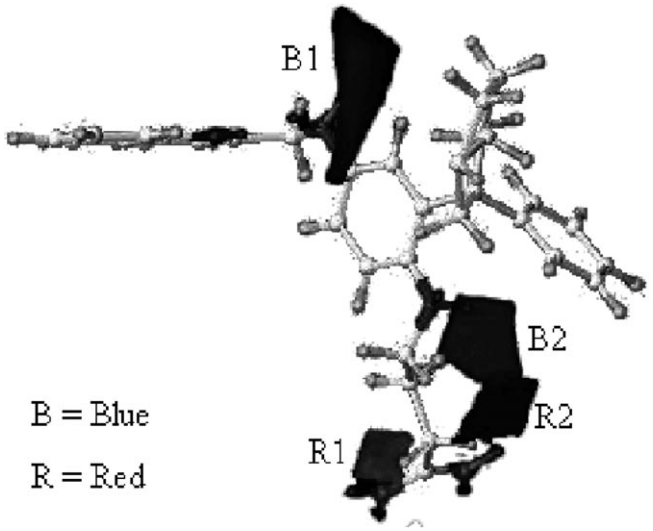

Figure 9. CoMFA electrostatic field distribution contour map in combination with inhibitor **12f.**

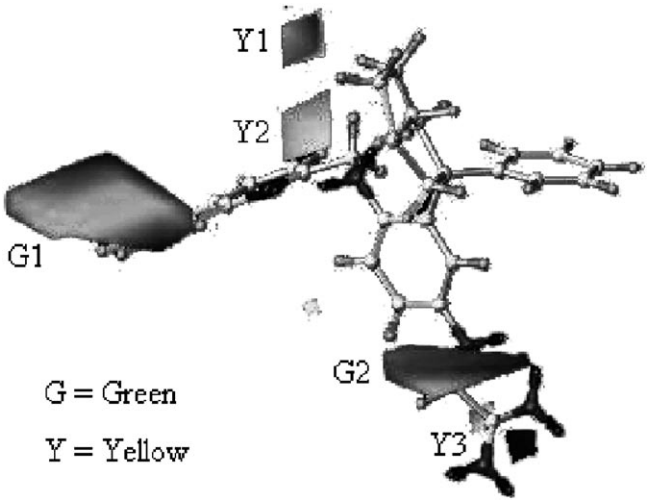

Figure 10. CoMFA steric field distribution contour map in combination with inhibitor **12d.**

due N23, D62, and T66 than pyridine. That is why the activity of compound **12l** is higher than compounds **12m**, **12n**, **12o**, and **12p.** The green contour G2 indicates that increased steric bulky substituents in this area are favorable for the inhibitory activities. This is in agreement with the fact that the inhibitory activity of compound **18c** with a bulky pyridine is higher than compounds **12g** and **12h.** There is a yellow contour Y3 below G2, which indicates that the steric bulky substituents must be appropriate. Compounds **18b** and **18f** have lower activities than compound **18c.** As shown in Figure 8, we can see there is a phenyl ring of **Phe25.** If bulky substitutes exist in these regions, the van der Waals interactions and space adoptions may be destroyed. This conclusion is compatible with the binding mode predicted by GOLD, which validates our docking result. In addition, there are two yellow contours Y1, and Y2 upon the molecule indicating that increased steric bulky substituents in this area are unfavorable for the inhibitory activities. Compounds **12b** and **12d** have low inhibitory activities, as illustrated in Figure 10, the R_2 substituent quinoline in the 5-position of the aryl is at the inner pocket of FLAP, and it is just in the opposite orientation of **18c** in Figure 8. The bicycloheptane ring is in the *ortho*-position, which forms close distances less than 3.0 Å between the bicycloheptane ring and Val21, Val20, Phe123, and Ile119 and the repelling force is enhanced, so it is unfavorable for the inhibitors to bind. Besides this, there is a blue contour B1 shown in Figure 9, which indicates negative charged groups are unfavorable for activity. The oxygen atoms of compounds **12b** and **12d** are closer to the phenyl ring of Ile119. Because of the high electron density around the phenyl ring of Ile119 and the lone-pair electrons of the oxygen atom, the repelling force is stronger. This is another reason why compounds **12b** and **12d** have lower activities. There are two red contours R1 and R2 in Figure 9 showing that more negative charged substituents are favorable. That is why compounds **12a**, **12c**, **12e**, **12f**, **12j**, **12k**, **18a**, and **18e** have high activities. As we know, the hydrogen in the NH group is electrophilic, further docking study showed that the NH groups of His28 and Lys116 might form H-bonds with the carbonyl, NMe_2, SO_2Me, or OH group in compounds **12a**, **12c**, **12e**, **12f**, **12j**, **12k**, **18a**, and **18e.** Moreover, the substituents containing carbonyl, NH, or OH group might also have strong electrostatic interactions with polar residues. There is a blue contour B2 upon red contour R_2, which indicates that positive charged groups is favorable; that is why the activities of compounds **12g** and **12r** are higher than **12s.** The R_2 substituent chains of the three compounds are too short to form H-bonds with His28 and Lys116, but compounds **12g** and **12r** with methyl groups can form weak hydrophobic interactions with Phe25, so they have higher activities.

We do not see obvious contours in the top right corner of Figure 8. The corresponding monocyclic 5 and 6-member ring compounds have similar potency to the bicycloheptanes, and the enantiomers (+)2 and (−)2 have similar activities [9]. As mentioned above, the bicyclic and monocyclic moieties are located in the hydrophobic region. Both the 5 and 6-member ring can form similar hydrophobic interactions with residues Val21, Val20, Phe123, and Ile119. That is to say, steric field contribution is dispensable there. It indicates that our CoMFA model is credible.

3.3 Validation of the 3-D QSAR Models

The six randomly selected compounds (Table 1) were used as the testing set to verify the constructed CoMFA model. The calculated results are listed in Table 2 and displayed in Figure 7. The predicted pIC_{50} with the QSAR model is in good agreement with the experimental data with a statistically tolerable error range and with a correlation coeffi-

Table 2. Summary of CoMFA analysis.

Parameter	CoMFA
Training set	–
PLS statistics	–
LOO	–
q^2 (CV correlation coefficient)	0.651
N (number of components)	4
SEP (standard error of prediction)	0.602
Uncross-validated	–
r^2 (correlation coefficient)	0.972
SEE (standard error of estimate)	0.169
F (F-ratio)	175.674
Field distribution	–
Steric	48.7%
Electrostatic	51.3%
Testing set	–
r^2 (correlation coefficient)	0.920
S (standard error of prediction)	0.298

cient of $r^2 = 0.920$ (Table 2). The testing results indicating that the CoMFA model would be reliably used in new inhibitor design for developing new FLAP inhibitors.

4 Conclusions

In this work, molecular docking and 3-D QSAR studies were carried out to explore the binding mechanism of substituted 2,2-bisaryl-bicycloheptanes to the FLAP. A good prediction CoMFA model was obtained with LOO cross-validation q^2 and conventional r^2 values of 0.651 and 0.972, respectively. The reliability of the model was verified by the compounds in the testing set. The docking/3-D QSAR results suggested that the quinoline and H-bond accepter in R_2 substituents with appropriate chain length are important for high activities, and both the 5- and 6-member rings can form similar hydrophobic interactions with residues Val21, Val20, Phe123, and Ile119. These results demonstrated the power of combining docking/QSAR approach to explore the probable binding conformations of compounds at the active sites of the protein target, and further provided useful information to understand the structural and chemical features of substituted 2,2-bisaryl-bicycloheptanes in designing and finding new potential FLAP inhibitors.0

References

[1] M. *Peters-Golden*, W. R. Henderson, *N. Engl. J. Med.* **2007**, *357*, 1841 – 1854.
[2] R. A. Lewis, K. F. Austen, R. J. Soberman, *New. Engl. J. Med.* **1990**, *323*, 645 – 655.
[3] C. D. Funk, *Nat. Rev. Drug Discov.* **2005**, *4*, 664 – 672.
[4] J. W. Woods, J. F. Evans, D. Ethier, *J. Exp. Med.* **1993**, *178*, 1935 – 1946.
[5] A. K. Mandal, J. Skoch, J. Brian, *Proc. Natl. Acad. Sci. USA* **2004**, *101*, 6587 – 6592.
[6] R. C. Murphy, M. A. Gijon, *Biochem. J.* **2007**, *405*, 379 – 395.
[7] R. N. Young, *Eur. J. Med. Chem.* **1999**, *34*, 671 – 685.
[8] M. Peters-Golden, C. Canetti, P. Mancuso, M. J. Coffey, *J. Immunol.* **2005**, *174*, 589 – 594.
[9] M. Dwight, B. Christine, F. Richard, *Bioorg. Med. Chem. Lett.* **2008**, *18*, 2023 – 2027.
[10] A. D. Ferguson, B. M. Mckeever, S. H. Xu, *Science* **2007**, *317*, 510 – 512.
[11] J. Gasteiger, M. Marsili, *Tetrahedron* **1980**, *36*, 3219 – 3258.
[12] M. D. Eldridge, C. W. Murray, T. R. Auton, *J. Comput. Aided Mol. Des.* **1997**, *11*, 425 – 445.
[13] C. A. Baxter, C. W. Murray, D. E. Clark, *Proteins* **1998**, *33*, 367 – 382.
[14] M. L. Verdonk, J. C. Cole, M. J. Hartshorn, *Proteins* **2003**, *52*, 609 – 623.
[15] M. C. Clark, R. D. Cramer, III., N. V. Opdenbosch, *J. Comput. Chem.* **1989**, *10*, 982 – 1012.
[16] B. L. Bush, R. B. Nachbar, Jr., *J. Comput. Aided Mol. Des.* **1993**, *7*, 587 – 619.

